

Contents lists available at ScienceDirect

### Icarus

journal homepage: www.elsevier.com/locate/icarus





# Daily and seasonal processes shape hydrological activity and detectability of moisture in Antarctic, Mars-analog soils

Ariel N. Deutsch<sup>a,1</sup>, Joseph S. Levy<sup>b,\*</sup>, James L. Dickson<sup>a,c</sup>, James W. Head<sup>a</sup>

- <sup>a</sup> Department of Earth, Environmental and Planetary Sciences, Brown University, Providence, RI 02912, USA
- <sup>b</sup> Department of Geology, Colgate University, Hamilton, NY 13346, USA
- <sup>c</sup> Division of Geological and Planetary Sciences, California Institute of Technology, Pasadena, CA 91125, USA

#### ARTICLE INFO

Keywords: Mars Brines Habitability Microclimate Antarctica

#### ABSTRACT

Soil salt deliquescence and soil porewater solution growth are key processes that generate potentially habitable conditions in hyperarid environments on Earth and could form near-surface pore waters on Mars, However, direct detection of soils darkened by saline porewater solutions on Mars has proven difficult owing to the limited number of imaging opportunities over potential brine-bearing sites, the limited diel temporal coverage of orbital sensors, and the diversity of spectroscopic properties of potentially brine-bearing substrates that limits direct detection of hydrated mineral phases. Here, we explore how these observational limitations would affect the interpretation of highly dynamic soil salt patches observed in the McMurdo Dry Valleys, Antarctica. These salt patches show daily and seasonal albedo change, darkening and brightening over timescales of minutes. Fully darkened conditions occur at a median surface relative humidity of 67.9  $\pm$  10.7%, while bright conditions occur at lower median surface relative humidity of  $38.9 \pm 14.5\%$ , leading to the interpretation that the albedo changes are caused by soil salt deliquescence and brine droplet growth. These humidity thresholds and the daily hysteresis between deliquesced and effloresced conditions are consistent with the properties of sulfate and chloride salts found at the site, but occur on timescales much faster than those observed under laboratory conditions (minutes vs. hours-days). Darkened soil patch conditions are most common between 21:00 and 06:00 local time, and are not detected during 78% of afternoon imaging opportunities, suggesting that episodic, afternoon satellite imaging would not be effective in resolving rapid albedo changes on similar planetary landscapes such as Mars. Instead, synoptic, high-cadence imaging is a more suitable remote sensing tool for evaluating albedo changes driven by surface salt deliquescence and efflorescence.

# 1. Introduction

On Earth, soil salt deliquescence (the absorption of atmospheric water vapor by soil salts that leads to dissolution of the salt grain) and soil solution growth (the continued absorption of water vapor into concentrated solutions when the vapor pressure of the pore solution is less than the partial pressure of water vapor in the air) are key processes that generate potentially habitable conditions in hyperarid environments (Davila et al., 2008, 2013; Gough et al., 2017) that are otherwise too cold or too dry to permit the widespread stability of soil porewaters (Levy, 2021). Hygroscopic salts have been detected on the martian surface, including chlorides (Osterloo et al., 2008) and perchlorates (Hecht et al., 2009; Smith et al., 2009). Such salts have been suggested to

be a possible source of local and transient liquid water on Mars under modern hyperarid conditions (Davila et al., 2010; Heinz et al., 2016). Salt efflorescence, deliquescence, and dissolution in soil pore waters produce pronounced changes in surface albedo (e.g., Craft and Horel, 2019). For that reason, martian hygroscopic salts have been proposed as a mechanism to explain surface darkening in recurring slope lineae (RSL) through either direct salt deliquescence (i.e., a wetting of the surface leading to a decrease in albedo), or through more complex mechanisms such as salt hydration and swelling or changes to soil cohesion during wetting and drying cycles leading to slope destabilization and soil movement (Bishop et al., 2021; McEwen et al., 2011; Schmidt et al., 2017; Wang et al., 2019; Gough et al., 2020). Other proposed mechanisms for RSL formation, such as dust avalanching and

<sup>\*</sup> Corresponding author.

E-mail address: jlevy@colgate.edu (J.S. Levy).

Now at: Planetary Systems Branch, NASA Ames Research Center, Moffett Field, California 94035, USA.

dust devil activity, may require no salts or liquids to be present (Edwards and Piqueux, 2016; Dundas et al., 2017; Stillman et al., 2020; McEwen et al., 2021).

Two major observational obstacles have led to the proliferation of hypotheses governing RSL formation—impacting both those that involve liquid water in RSL formation and those that do not. The first is the limited number and limited diel coverage of RSL sites by the High Resolution Imaging Science Experiment (HiRISE) over the course of the martian summer during which RSL lengthen. The limited snapshots of RSL change have all been collected during martian local afternoon (McEwen et al., 2010), and together, provide a time-transgressive view of RSL change that is broadly consistent in terms of surface change rate and morphology with RSL growth via the flow of subsurface fluids through granular regolith (Grimm et al., 2013; Huber et al., 2020; Lark et al., 2021; Levy, 2012; Stillman et al., 2016; Tebolt et al., 2020). The second major challenge is the difficulty in determining the composition of RSL and RSL-supporting slopes via reflectance spectroscopy. Hydrated salts have been reported at RSL sites (Ojha et al., 2015), however, these sites are all locations of high spectral diversity, which can lead to anomalous detections of absorption features near 1.9 and 2.1 µm (Leask et al., 2018). Additionally, the Compact Reconnaissance Imaging Spectrometer for Mars (CRISM) has a relatively large spatial footprint even when used to make targeted measurements with gimballed motion (~12 m; Murchie et al., 2007) in comparison to the small, dynamic meter-length scales associated with albedo changes in RSL. Put succinctly, the number of observations of RSL sites is limited by orbital imaging constraints (despite aggressive repeat imaging campaigns), the timing of those observations is fixed by the Mars Reconnaissance Orbiter orbit, and the presence or absence of hydrated phases at RSL sites is ambiguous.

Here, we explore how these observational limitations would change the interpretation of highly dynamic, albedo-changing soil salt patches observed in the McMurdo Dry Valleys, Antarctica, where hypersaline and hyperarid landscape processes are comparatively well understood across yearly to interannual time scales. The water budgets of hyper-arid landscapes are well characterized, but are typically evaluated over daily to seasonal time scales (e.g., Davila et al., 2013; Gooseff et al., 2003, 2017; McKay et al., 2003). Likewise, the deliquescence behavior of salts is well characterized in the lab, with complete phase transitions observed to occur over hours to days (Gough et al., 2017; Heinz et al., 2016; Nuding et al., 2014; Sato and Hattanji, 2018; Tang and

Munkelwitz, 1993; Yang et al., 2006). A hysteresis in the deliquescence relative humidity (DRH) and efflorescence relative humidity (ERH) at which salt phase changes occur are well described in both lab and field settings (Sato and Hattanji, 2018; Zehnder and Schoch, 2008). Finally, the distribution of hygroscopic salts in many arid environments is well known, based on soil sampling and subsequent laboratory analysis (Bisson et al., 2015; Claridge and Campbell, 1977; Davila et al., 2008, 2013; Keys, 1979; Keys and Williams, 1981).

Despite these major advances in our understanding of hyperarid environments, fewer studies consider the non-equilibrium rates of salt deliquescence and soil solution growth (e.g., Dai et al., 2016; Dickson et al., 2013; Gough et al., 2017; Levy et al., 2012). Under conditions of rapidly-changing relative humidity (RH) and temperature, soil salts can deliquesce and pore solutions can grow to darken soils, potentially over rapid timescales of only minutes to hours, as complex mixtures of soil salts interact with atmospheric water vapor.

Here we report on rapid (tens of minutes) albedo changes in soil salt patches in the McMurdo Dry Valleys of Antarctica. We evaluate whether these albedo changes are driven by cyclic daily and seasonal RH changes at the soil-atmosphere interface. Specifically, we analyze episodes of brightening and darkening of soil salt patches at the Garwood Valley ice cliff site (Fig. 1) using time-lapse images acquired every five minutes over three austral summer field seasons. We then correlate these episodes of albedo change with RH and surface temperature collected at a cliff-adjacent meteorological station. By analyzing high temporalresolution imaging and in situ meteorological data, we seek to understand the microclimate drivers that might control the direction of albedo changes (light to dark or dark to light) and the duration of albedo changes. Finally, we discuss geological interpretations that could be drawn using only late afternoon observations of the field site (comparable to orbital imaging campaigns of the martian surface) to determine how temporally-limited imaging efforts affect measurements of albedo change interpreted to result from rapid changes in soil moisture. We evaluate how the temporal resolution of the remote sensing tool used to detect albedo changes might change the interpretation of those albedo changes, using salt expression in Antarctica as a terrestrial analog for potential deliquescent soil salt features on Mars.

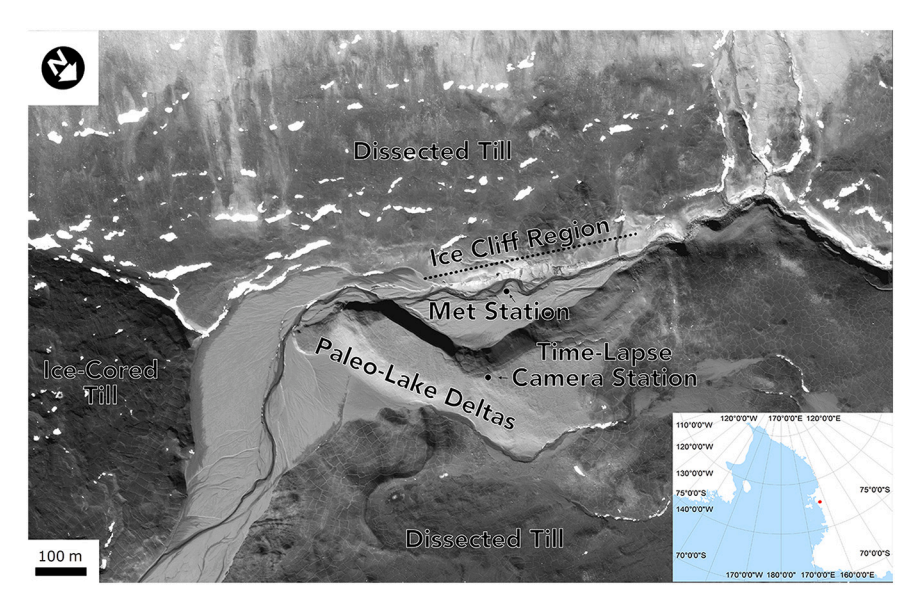


Fig. 1. Site map showing the Garwood ice cliff location as well as the micrometeorological station (Met Station) and the time-lapse imaging station. Inset map shows the location of Garwood Valley in the Ross Sea region of Antarctica. Base map is portion of worldview image WV02\_20131212203053\_103001002A5A4700, courtesy the Polar Geospatial Center.

#### 2. Methods

#### 2.1. Field setting

Time-lapse imaging (section 2.2) and micrometeorological observations (section 2.3) were collected at the Garwood Valley ice cliff (78°S, 164°E), located in the McMurdo Dry Valleys (MDV) of Antarctica (Fig. 1). Garwood Valley is located in the coastal thaw zone (CTZ) of the MDV and is characterized by low levels of precipitation (<80 mm of water equivalent per year from snowfall largely lost to sublimation), low temperatures (mean summertime of  $\sim-5$ °C, mean daily maximum of  $\sim-2$ °C), and relatively high RH (~64%) (Marchant and Head, 2007, Fountain et al., 2014, Fountain et al., 2009, Schwerdtfeger, 1984). The RH mean is high compared to other MDV sites and is attributed to prevailing winds that transport moisture from the Ross Sea at the mouth of the valley.

The ice cliff site is a cut-bank in Pleistocene-aged, ice-cored till caused by incision and undercutting of the Garwood River into underlying glacial deposits (Levy et al., 2013; Levy et al., 2017). Although called the ice cliff due to widespread observations of buried glacier ice outcrops from ~2011 to 2014, rapid thermokarstic subsidence has led to the release of overlying dry sediments and near-complete covering of exposed ice to form ice-cored talus cones and a sediment-surfaced hill-slope. The hillslope is crosscut by small gullies (Levy et al., 2013) and has numerous surface salt patches (described in detail in Bisson et al., 2015), composed primarily of a mixture of euhedral sulfate salts (mirabilite and thernardite) in a matrix of subhedral halite.

In the hyperarid, hypothermal environment of the MDV, surface salts are deposited from a variety of sources (Bao and Marchant, 2006; Bisson et al., 2015). Salts deposited by precipitation of snow typically become concentrated at the site of deposition because rates of evaporation and sublimation exceed precipitation (Marchant and Head, 2007). Salts released from the weathering of rocks and soils tend to accumulate continuously in the soils (Levy et al., 2011; Marchant and Head, 2007; Toner et al., 2013; Toner and Sletten, 2013) unless they are flushed by surficial streamflow (Ball and Levy, 2015) or saturated hyporheic exchange (Gooseff et al., 2003). In some cases, mixtures of shallow groundwater and surface water have mobilized salts in MDV water tracks, resulting in saline pore water solutions and brines that commonly discharge as seeps near the valley floor (Ball and Virginia, 2012; Harris et al., 2007; Lyons et al., 2005). The vertical migration of water through soils can also mobilize and concentrate salts (Dickinson and Rosen, 2003). Regardless of the deposition mechanism, concentrated soil salts can result in seasonal variations in soil moisture, including isolated "wet patches" (Levy et al., 2012) and hillslope salty deposits containing unfrozen pore waters at below-freezing temperatures (e.g., Claridge and Campbell, 1977).

Soluble salts like those present across the MDV commonly deliquesce when the atmosphere is sufficiently humid, with each salt species or mixture of salt species undergoing phase change at a specific DRH and efflorescing at a lower ERH. The specific RH values depend on the species of the salt and the surface temperature. The DRH is typically lower for mixtures than it is for pure phases (Tang and Munkelwitz, 1993; Yang et al., 2006).

When salts deliquesce at the soil surface, moisture darkens the sediments as pore waters grow and then coat soil and salt grains, resulting in a lowering of albedo (e.g., Levy et al., 2012; Dickson et al., 2013; Massé et al., 2012). Different materials potentially present in time-lapse imaging scenes vary in albedo, from bright snow (0.8–0.9) to crystalline hydrated halite (0.6–0.9, falling to 0.3 for dissolving conditions), with sulfates having intermediate albedos over visible wavelengths, e.g., thenardite (0.7), mirabilite (~0.85), and anhydrous halite having a similar albedo (~0.85) (Carns et al., 2016).

Contrastingly, salts migrate to the surface of a porous material during efflorescence, and the resulting coating of salts can commonly be identified by the increase in albedo. Over the course of austral summer,

episodes of salt efflorescence have also been observed in the field (e.g., (Bisson et al., 2015; Claridge and Campbell, 1977; Keys and Williams, 1981; Nishiyama and Kurasawa, 1975). On shorter timescales, Dickson et al. (2013) documented dynamic examples of deliquescence and pore solution growth occurring in the MDV using time-lapse observations and measurements of RH obtained from near a valley thalweg water track east of Don Juan Pond, in neighboring Wright Valley. They demonstrated that deliquescence and brine growth are active processes within the Don Juan Pond watershed, and prompted questions about the frequency, distribution, and duration of these processes. Outside of concentrated soil salt hotspots, soil porewater solutions in the MDV grow and shrink on diurnal timescales, darkening soils during high RH events and brightening them during typical, low-RH periods (Levy, 2021).

#### 2.2. Time-lapse methods

Time-lapse images were acquired every five minutes at the Garwood ice cliff site over the course of three austral summer field seasons. These images were acquired with Canon Powershot a590 IS digital camera with firmware-modifications that enabled time-lapse imaging using the system clock as an intervalometer. Images were acquired from 10 Jan 2012 through 28 Jan 2012 (1717 total images), from 13 Dec 2012 through 9 Jan 2013 (2592 total images), and from 4 Jan 2015 through 3 Feb 2015 (2878 total images). Images were automatically synchronized with meteorological measurements to allow instantaneous direct comparisons between meteorological forcing and any observable surface response (Dickson et al., 2014).

While the whole ice cliff site was imaged (Fig. 2), we largely focus our analysis and discussion on a representative,  $\sim$ 5 × 5 m salt patch on the soil-covered slopes of the cliff. Two methods were used to evaluate surface change of the soil salt patch, qualitative image classification and quantitative image brightness level analysis. For qualitative analyses, each image was manually inspected for a change in relative albedo (Fig. 3), and was classified into one of five categories: (1) dark, (2) bright, (3) both dark and bright regions present, (4) snow covered, or (5) indeterminate activity/inactive (Fig. 3). For quantitative image brightness level analysis, each image was cropped to the salt patch region of interest, and then mean DN (digital number) brightness level across the red, blue, and green image channels was determined for all pixels in salt patch sub-image. The mean salt patch DN was then ratioed to the maximum DN value in the full image in order to normalize brightness of the salt patch region of interest to overall scene brightness (effectively taking the comparatively high and comparatively consistent albedo of fresh and sublimating snow banks as standard between images). We report soil salt patch brightness as mean normalized DN, which has a value ranging from 0 (no signal on the camera detector) to 1 (brightness equal to the brightest pixel in the time lapse image).

#### 2.3. Meteorological station data

Time-lapse images were compared to RH and temperature measurements collected at a long-term weather station located  $\sim\!100$  m from the soil salt patch (Fig. 1) and  $\sim\!10$  m from the ice cliff slope. The station is located on the braid plain of the Garwood river, in front of the ice cliff site cutbank, and experiences nearly identical illumination to the ice cliff. Meteorological measurements were collected using sensors connected to a Campbell Scientific CR10X datalogger. Surface temperature was measured using an Apogee Instruments SI-111 infrared radiometer (instrument intrinsic maximum measurement uncertainty of  $\pm0.2~^{\circ}\mathrm{C}$  with emissivity variability generating <2% error). Air temperature and RH at 3-m elevation were measured using a Vaisala HMP60 probe (instrument intrinsic maximum measurement uncertainty of <5%). All measurements were logged at 15-min intervals. Data are available for download at www.mcmlter.org.

Micrometeorological data for the three field seasons were processed



**Fig. 2.** Salt patch brightening and darkening behavior across the ice cliff site is synchronous between patches. Image field-of-view is 100 m. Dotted box shows the focus area in Fig. 3.

to determine how albedo change relates to surface classification and mean normalized DN. In order to correct for differences between air temperature on the 3 m tall weather station mast and air temperature in the pore spaces of the soil salt patch, RH data were reprocessed to determine the equivalent RH for air in contact with and in thermal equilibrium with the cliff soil surface (after Levy, 2021), here termed soil RH. Soil RH was calculated by determining total atmospheric vapor pressure measured at 3-m elevation (RH times saturation vapor pressure for air temperature recorded at 3 m) using the Magnus equation in the Huang (2018) formulation, and then determining the saturation vapor pressure for air in equilibrium with the soil surface temperature. Soil RH is the ratio between the water vapor pressure measured at 3 m elevation and the saturation vapor pressure of air that has the same temperature as the soil surface:

Soil RH = 
$$(p_{vap,3m})/(p_{vap,sat,ground})$$
 (1)

where  $p_{vap,\;3m}$  is water vapor pressure measured at 3-m elevation and  $p_{vap,sat,ground}$  is the saturation vapor pressure for air at the same temperature as the soil surface. All scripts used to process raw .csv-formatted data can be found at: https://github.com/jslevy/garwood\_albedo

#### 3. Results

#### 3.1. Albedo change over time

Across the Garwood ice cliff, salt patches are abundant and alternate between a low-albedo state and a high-albedo state (Fig. 2, Supplementary Material, A). These albedo-changing patches are located exclusively along the slope of the cliff and are absent from surrounding hillslopes and paleo-delta surfaces (Fig. 1). They are found in isolation along the cliff slope, on interfluves between gully channels, and within gully depositional fans (Fig. 2). The patches change albedo synchronously (Fig. 2), such that all patches visible in the time lapse imaging frame are in either low- or high-albedo states at the same time. The patches change between albedo states at broadly similar rates, although some patches are slower than other proximal patches to fully change albedo. Although slower, these patches typically only lag by one time-lapse frame (5 min). Across imaging years, slower patches are consistently slower to change albedo.

To analyze the relationship between the salt activity and environmental conditions, we focus on a  $\sim 5\times 5$  m salt patch that is taken to be representative of the albedo-changing patches across the ice cliff site based on the near synchronicity of albedo change observed across the site (Figs. 2-3). Variations in surface state (fully dark, fully bright, both bright and dark, snow-covered, or indeterminate) are temporally correlated with variations in RH (Fig. 4-5). The patch shows temporally contiguous episodes in each season when each surface state persists for hours to days. The number and duration of surface state episodes are reported for each field season in Table 1.

For all field seasons, fully dark episodes occurred more frequently than fully bright episodes, although fully dark episodes were shorter-lasting (Table 1). Simultaneous bright and dark albedo conditions (catalogued as "both") commonly occurred between episodes of fully bright or fully dark conditions. Snowfall events occurred in all field seasons, obscuring the salt patch. Snowfall was typically followed by a period of dark albedo, or by a transitional period of indeterminate activity (Table 1).

# 3.2. Relative humidity, temperature, surface brightness, and surface classification

Surface RH follows a diurnal cycle at the site, oscillating between  $\sim$ 25% and 95%, and also shows secular change over the measurement season, drying out towards the end of the January imaging campaign

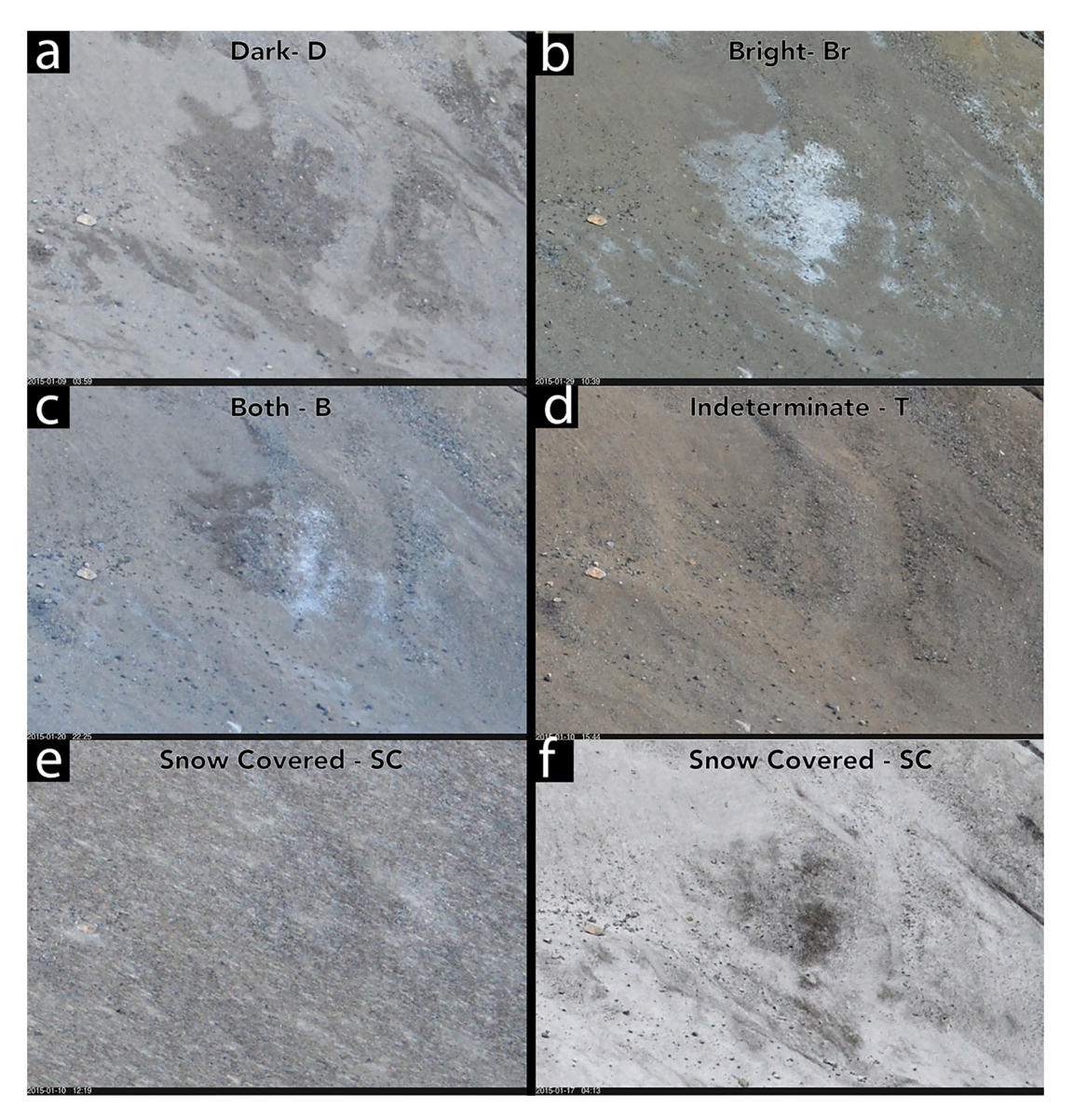


Fig. 3. Type examples of surface characterization states used to interpret time lapse images.

(Fig. 4-5). Surface RH values are commonly lower than air RH values owing to the warmer temperature of the soil surface in comparison to the air temperature. The salt patch darkens on the rising limb of surface RH, stays dark through peak RH, and then turns bright several RH percentage points lower than darkening began during the wetting phase. The salt patch stays bright through minimum daily RH, and then darkens again during the rising RH period (Fig. 5). A hysteresis is present in the surface classification data (Fig. 4).

Each salt patch surface condition classification is associated with a range of surface RH and temperature conditions recorded at the adjacent met station (Figs. 4, 6-8). All values listed here are reported with one standard deviation uncertainty values to provide an indication of data central tendency. Fully bright and fully dark conditions are contrasted, as conditions with both bright and dark portions of the salt patch have intermediate values between these extremes (Figs. 7-8).

Bright conditions occur at a median surface RH of 38.9  $\pm$  14.5%, while fully dark conditions occur at a median surface RH of 67.9  $\pm$  10.7%. Bright conditions occur at a median surface temperature of 0.6  $\pm$  4.6 °C, while dark conditions occur at a median temperature of -0.4 °C  $\pm$  2.0 °C. The temperature difference (surface temperature minus air temperature) during bright periods is 1.3  $\pm$  3.2 °C versus 0.9

# $\pm$ 1.6 °C for dark periods.

The differences between surface RH and temperature for different surface conditions are statistically significant (Figs. 7-8), based on a Wilcoxon unpaired comparison of means test (used for comparison of two non-normally-distributed groups, for example, RH data that has inbuilt skewedness owing to the limits of the RH scale). The largest and most significant difference is between RH for bright and dark surface conditions (p < 2.22e-16), while small but significant differences in RH exist between fully bright and both bright and dark surfaces (p = 8.9e-6). A small, but significant difference exists between surface temperatures during dark and bright conditions (p < 2.22e-16). The temperature difference between dark and both bright and dark conditions is only marginally significant (p = 0.041).

#### 4. Discussion

What is causing the brightening and darkening of the soil salt patch? One possibility is that apparent brightening and darkening detected and described in the qualitative surface classification dataset is due entirely to photometric effects (i.e., the surface appears brighter when the sun is directly behind the camera and darker then the sun is directly behind the

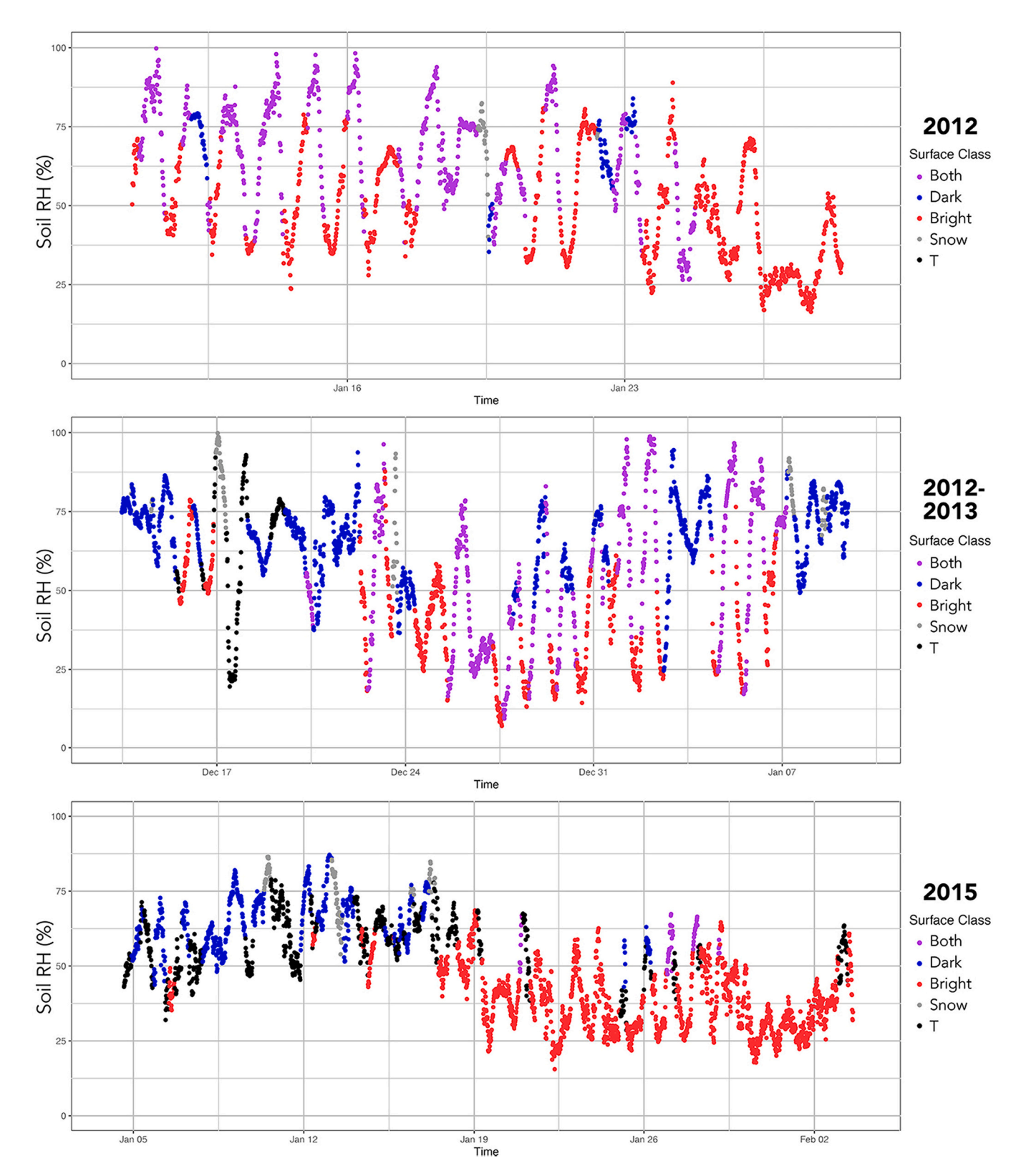


Fig. 4. Surface state and soil surface relative humidity over the three study periods. Both indicates both bright and dark patches present, Dark indicates fully darkened patches, Bright indicates fully brightened patches, Snow indicates snow-cover, and T is indeterminate. The salt patch shows dark conditions and high RH, bright conditions and low RH, diel and seasonal cycling between dark and bright, and hysteresis in the RH threshold at which albedo change occurs.

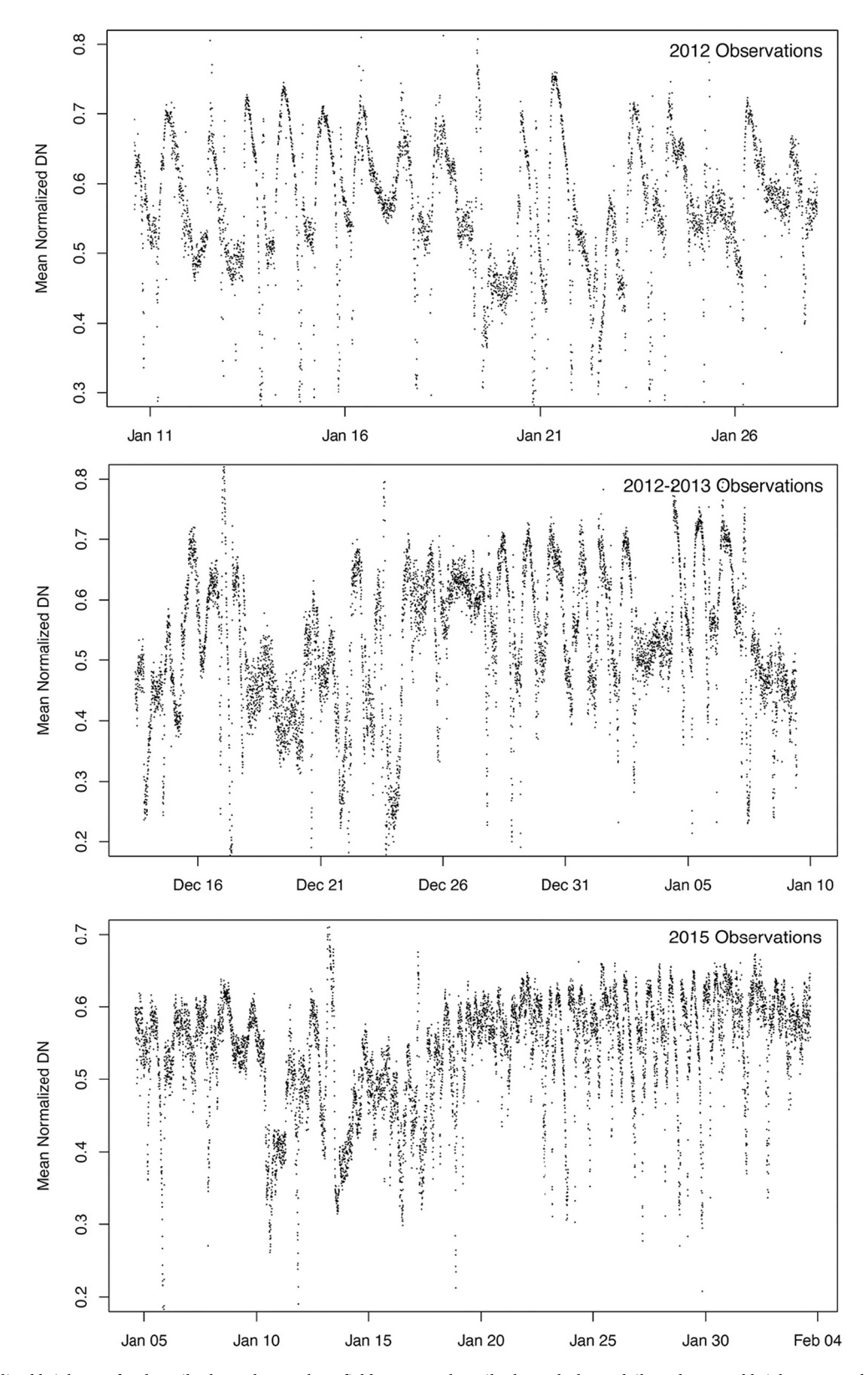


Fig. 5. Mean normalized brightness for the soil salt patch over three field seasons. The soil salt patch shows daily and seasonal brightness trends, with cyclic changes in brightness over most days, and secular changes in brightness with overall bright or dark mean conditions persisting over different parts of the summer season.

soil salts). The azimuth from ice cliff soil salts to the time-lapse camera station is 75° clockwise from north. Accordingly, the sun is at opposition around 08:00 local time. The time when the soil salt patch is brightest on a typical day occurs near noon local time (Fig. 9), and not near 08:00 local time, when the sun is in opposition to the ice cliff, relative to the

time lapse camera (Fig. 1).

In addition, at opposition apparent reflectivity may be greater for surfaces in the image data, however, it will be greater for all parts of the image. The rise and fall of the average mean DN for the salt patch relative to all other pixels in the time-lapse image field of view means

**Table 1**Classification of activity types on the Garwood Ice Cliff during the three studied field seasons.

Field Season	Type of activity	Indeterminate	Snow covered	Dark	Bright	Both
10 Jan 2012–28 Jan 2012	Number of episodes	0	2	13	5	15
	Range of duration of episodes (hrs)	0	0.5-6.25	4.25-36.5	7.75-162	1.75-36.5
	Mean duration of episodes (hrs)	0	3.60	14.5	78.5	10.8
13 Dec 2012–9 Jan 2013	Number of episodes	5	6	21	11	17
	Range of duration of episodes (hrs)	1.75-19	0.5-9	7.5-66	1.75-87	0.25-39.75
	Mean duration of episodes (hrs)	7.85	4.21	20.7	27.8	9.65
4 Jan 2015–3 Feb 2015	Number of episodes	29	6	20	14	4
	Range of duration of episodes (hrs)	1-29.5	0.25-10.5	1-42.25	0.5-117	1.25-6.5
	Mean duration of episodes (hrs)	6.02	3.79	7.96	26.9	3.75

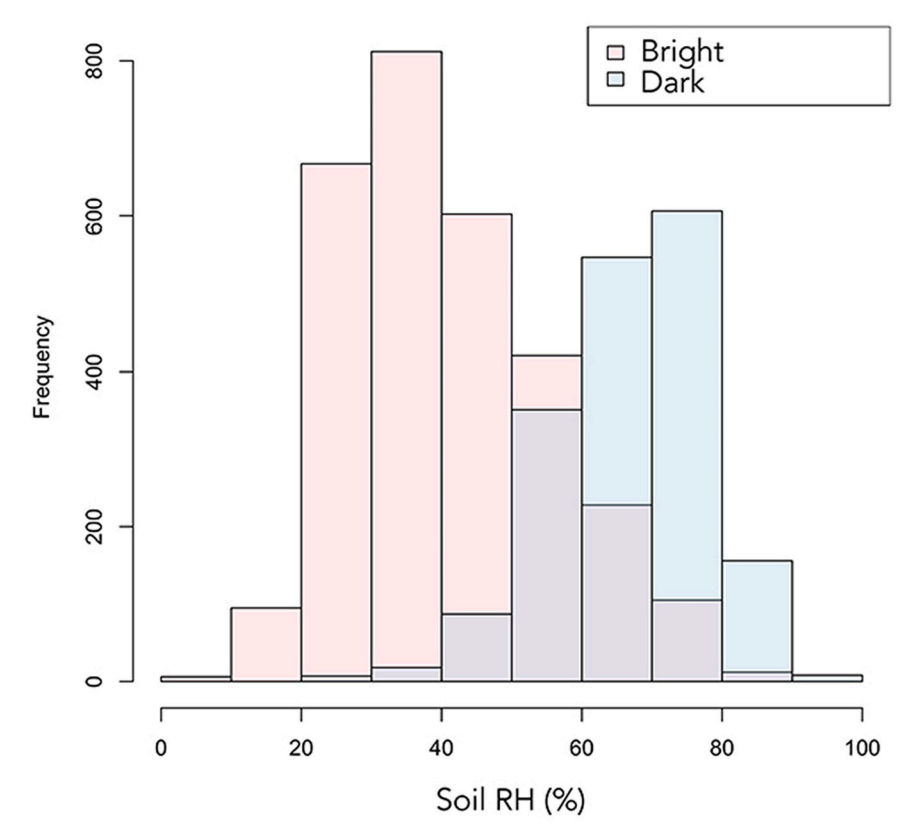


**Fig. 6.** Histograms of RH conditions for bright and dark patch states. Darkening occurs at high soil RH, typically above ∼50%, while bright conditions occurs at low soil RH, typically below ∼50%. Purple-shaded areas show overlap between humidity during bright and dark conditions. Above 60% RH, purple bars show the frequency of bright conditions (i.e., dark is more common at these RH values, but some images included bright surface states), while below 60% soil RH, bright conditions are more common and purple bars show the frequency of dark conditions. (For interpretation of the references to colour in this figure legend, the reader is referred to the web version of this article.)

that it is darkening and brightening relative to the surface that is on. For these reasons, we discount illumination variation as the primary direct driver of change of surface brightness in the time lapse image data.

The strong coupling between surface RH and surface state (bright, dark, or both) suggests that atmospheric processes related to water vapor may be driving the albedo changes observed at the ice cliff site. Indeed, quantitative measures of soil salt patch brightness (mean DN) are correlated with soil relative humidity; across all years and all measurements; as moisture levels rise in the air above the soil, the brightness of the soil salt patch drops (Fig. 10). We interpret this correlation between relative humidity and surface brightness to indicate deposition of atmospheric water vapor into the ground surface, either as soil salts deliquesce and/or as low-water-activity soil brine droplets grow.

However, several questions are raised by this dataset and analysis: (1) What salts are present at the Garwood ice cliff site? (2) Are the deliquescence and efflorescence of these salts consistent with the observed surface RH patterns? (3) Are mechanisms beyond deliquescence and efflorescence contributing to surface albedo changes at the site? And (4) how might these observations bear on the interpretation and analysis of RSL, or other putative groundwater features in planetary environments?

4.1. What transiently dark and bright salts are present at the Garwood Valley ice cliff?

Hygroscopic salts are common in the MDV and are abundant in Garwood Valley (Claridge and Campbell, 1977; Bisson et al., 2015). Large blocks of mirabilite (Na<sub>2</sub>SO<sub>4</sub>·10H<sub>2</sub>O), a hydrous sodium sulfate mineral, have been described in Ross Sea Drift till deposits in the mouth of Garwood Valley (Stuiver et al., 1981), resulting from freeze-drying of marine fluids trapped by the grounded ice sheet during the last glacial maximum. More recently, Bisson et al. (2015) collected salts from the Garwood Valley ice cliff site and identified mirabilite along with thenardite (Na<sub>2</sub>SO<sub>4</sub>), the anhydrous phase of sodium sulfate along with ~25% by mass chloride salts dominated by NaCl. In sodium sulfate evaporation experiments, mirabilite and thenardite have also been shown to coexist with metastable Na<sub>2</sub>SO<sub>4</sub>(III), suggesting the possibility that other sulfate phases may be present (Rodriguez-Navarro and Doehne, 1999). In the MDV, sulfates can be introduced by wind-blown sea salt, chemical weathering, marine incursion, hydrothermal processes, or oxidation of biogenic sulfur in the atmosphere (Bao and Marchant, 2006), while sodium chloride deposition is dominated by modern marine aerosols (Bisson et al., 2015). The three major

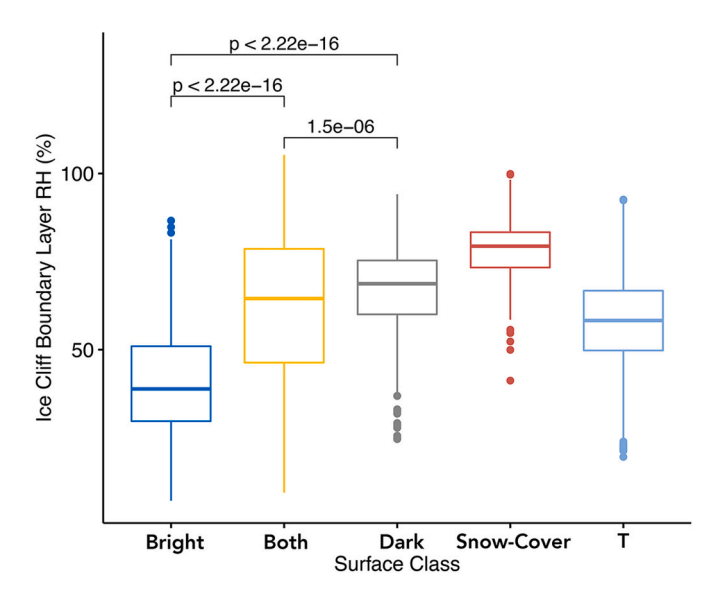


**Fig. 7.** Box plots showing the range and median values of RH under which different surface conditions are observed. Bright conditions are dominated by low RH conditions at the ice cliff, while dark conditions are associated with high ground-level RH. T indicates indeterminate.

components of the soil sulfate budget (sea-salt sulfate, non-sea-salt sulfate, and background sulfate derived from weathering and volcanic sources) vary as a function of elevation and distance from the coast (Bao and Marchant, 2006). Thus, while the particular albedo-changing salt patch focused on in this investigation (Fig. 3) has not been sampled in the field, salt patches along the ice cliff study site that undergo albedo change synchronously with this patch have been sampled by Bisson et al. (2015) and are composed of sulfates (mirabilite and thenardite) in a halite matrix.

4.2. Are the deliquescence and efflorescence characteristics of the salts present at the Garwood ice cliff site consistent with the observed brightness/humidity patterns?

The correlation between salt patch surface state (Fig. 4) and RH suggests that deliquescence and efflorescence are the dominant phase changes associated with albedo change at the site. At 0 °C, the DRH for mirabilite is 98.8%, the DRH for thenardite is 84.4%, the DRH for metastable  $Na_2SO_4(III)$  is 79.9% (Steiger and Asmussen, 2008) and the DRH for NaCl is  $\sim$ 75–80% (Koop et al., 2000; Wise et al., 2012). These DRHs decrease slightly (1–2 humidity percentage points) when the salts are warmed to temperatures observed at the field site (typically <10 °C). During evaporation and precipitation, sodium sulfate solutions can precipitate all three mineral phases, with anhydrous thenardite dominating when RH is below 50%, and decahydrated mirabilite dominating when RH is above 50% (Rodriguez-Navarro and Doehne, 1999). Efflorescence occurs at lower RH than deliquescence (Tang and Munkelwitz, 1993), with thenardite efflorescing at 55% RH (Martin, 2000) and NaCl efflorescing at  $\sim$ 40–45% (Koop et al., 2000; Wise et al., 2012).

These ranges of thermodynamically-predicted and/or experimentally-determined DRH and ERH are broadly consistent with the range of surface RH values measured at the ice cliff site. Dark soil conditions were observed between measured humidity values of  $\sim\!20\text{--}100\%$  (median: 67.9%), while effloresced conditions prevailed during observation periods with RH values of  $\sim\!0\text{--}80\%$  (median: 38.9%). Broadly, wetted (deliquesced, or both deliquesced and effloresced) conditions were common when surface RH exceeded 50%, and dry (effloresced) conditions were common when surface RH was lower.

The hysteresis observed in the surface state is also consistent with efflorescence processes. Soils darkened during rising RH conditions, but then only became brighter when RH values fell below the RH at which darkening began (commonly by 10–20 RH percentage points). This is consistent with the observation that other salts in MDV soils such as chlorides exhibited lower ERH values at high temperatures and higher ERH values at low temperatures (Gough et al., 2017). As the ice cliff soils warm in the morning and afternoon, increasingly low RH values may be needed in order to cause salt efflorescence.

Accordingly, we interpret albedo change at the ice cliff site to be

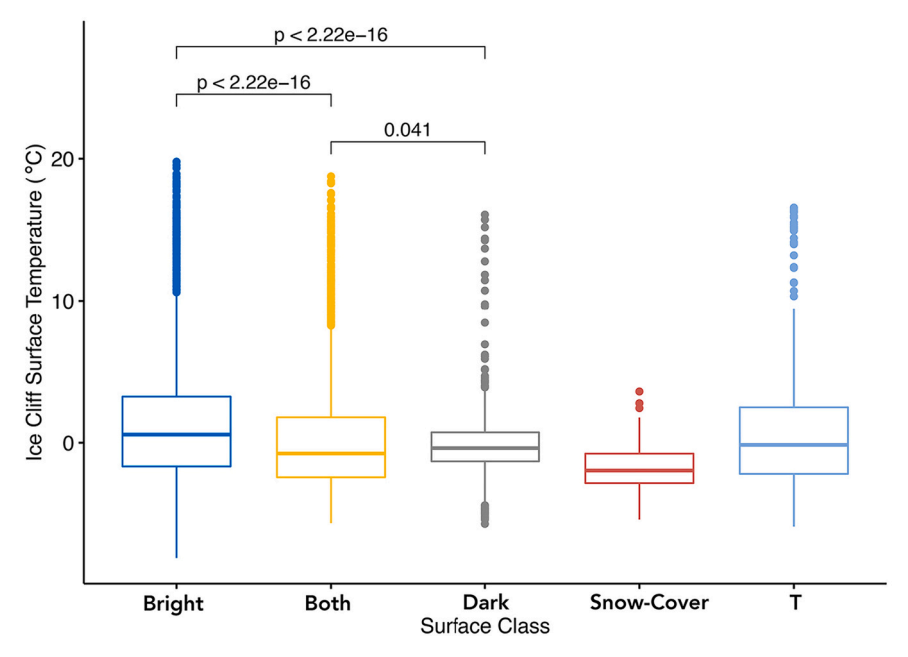


**Fig. 8.** Box plots showing the median, 25th and 75th percentiles, range (defined as 25th percentile minus 1.5 times the inter-quartile range and 75th percentile plus 1.5 times the interquartile range), and outlier values of temperature under which different surface conditions are observed. Bright occurs under slightly warmer temperatures than Dark, with conditions with both bright and dark patches occurring at intermediate temperatures. T indicates indeterminate.

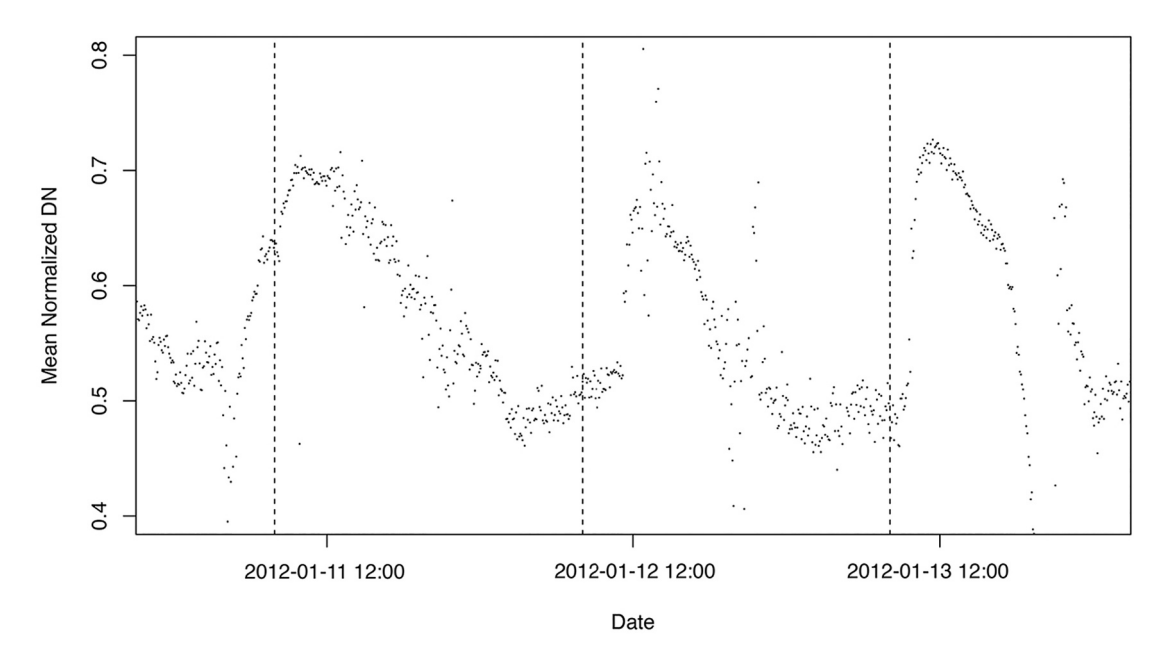


Fig. 9. Soil salt patch mean normalized DN over the course of three typical, mostly sunny days. The maximum brightness for the soil salt patch occurs near to shortly after noon local time and not close to 08:00 local time (dashed lines) when the sun is in opposition to the ice cliff relative t the camera station.

caused by the repeat deliquescence and efflorescence of surface salt patches. The mixture of sulfate and chloride salts along the ice cliff may explain some of the heterogeneity in behavior observed on the salt patch. For example, the persistence of both bright and dark portions of the patch as RH rises in the evening may be explained by the low DRH of NaCl and the comparatively higher DRH of the sulfates. In this process model, chlorides would deliquesce early in the evening, beginning the darkening process, while sulfates remain effloresced. As RH rises and as brine droplets grow, sulfates deliquesce and/or dissolve in the growing pore water droplets, transitioning the patch from both bright and dark to fully darkened. As RH falls in the morning, less hygroscopic sulfates may effloresce first, initiating growth of the bright patch, with NaCl efflorescing as RH approaches its daily minimum.

The repeat time-lapse imaging campaigns at the Garwood site provide the first measurements of the rate of change in surface albedo of salt patches in a field sedimentary setting. Previously, most studies on the timing of deliquescence and efflorescence have been in the laboratory or in slowly-changing built structures (e.g., stone buildings). Most studies have focused on chloride salts, which deliquesce and effloresce readily at low RH (Gough et al., 2017; Tang and Munkelwitz, 1993). At temperatures relevant to Antarctic salt patches and RSL sites during martian summer, the deliquescence of chloride hydrates occurs within hours or days (Wang et al., 2019), consistent with the growth of soil solutions in MDV soils over hours to days when exposed to high RH laboratory conditions (Levy et al., 2014; Heinz et al., 2016). The rates of albedo change observed in our time-lapse images of the MDV are faster than those observed in such laboratory experiments.

What could be causing the rapid change in soil salt state at the Garwood site? It is possible that it is related to the differences in salt composition, or salt mixtures, and thus differences in salt-specific DRH. Alternatively, it is possible that this is related to external factors that are introduced outside of a laboratory setting, such as lower and non-fixed temperatures. Importantly, Heinz et al. (2016) found no experimental correlation between the salt's DRH value and the Tv of a salt and soil mixture (Tv is the time after exposure to high RH at which the beginning of deliquescence could be observed visually). The apparent persistence of partially effloresced salt patches during the rising limb of RH oscillations and the persistence of wetted soils down to humidity values below the predicted ERH, are broadly consistent with the variable time lag between RH forcing and albedo response.

4.3. Are mechanisms beyond deliquescence and efflorescence contributing to surface albedo changes at the site?

Beyond deliquescence and efflorescence, other factors may also be playing a role in albedo change. For example, albedo change could result not from the deliquescence phase change (solid to brine at the salt grain scale), but instead from growth of brine droplets when atmospheric RH exceeds the water activity of the porewater solution. This process is used to explain the strong correlation between peak humidity levels and visible surface effects in chloride salt water tracks at Don Juan Pond, where features rapidly (over minutes) darkened when exposed to moist air (Dickson et al., 2013). At the Garwood site, growth of these brine droplets could lead to further dissolution of effloresced soil salts, rapidly darkening the surface.

Alternatively, phase change between anhydrous thenardite and hydrated mirabilite could be occurring as RH rises. At 0  $^{\circ}$ C, thenardite will transition to mirabilite when RH exceeds 60.6% (Rodriguez-Navarro and Doehne, 1999). However, at visible wavelengths, mirabilite is  $\sim$ 25% more reflective than thenardite (Carns et al., 2016). If hydration-dehydration of the sodium sulfate were the only process at work at the ice cliff, we would expect to see the opposite sense of change to what is observed: high albedo at high RH and low albedo at low RH. Instead, the opposite occurs, suggesting that hydration of sulfate minerals is not controlling the daily cycle of albedo change.

Transformation from bright, hydrated mirabilite to lower albedo anhydrous thenardite could explain the transitions from wetted to indeterminate albedo observed at several points throughout the imaging campaign (Fig. 4). As mirabilite that was initially formed during efflorescence or evaporative crystallization at high RH dehydrates to thenardite at low RH, the albedo of the soil crust could darken to values approaching that of surrounding, low-salt soils, resulting in disappearance of the salt crust bright patch. Intriguingly, given that hydrated salts deliquesce at higher DRH than anhydrous salts (Nuding et al., 2014), such a mirabilite to thenardite phase transition might prime the patches for future wetting events by lowering the RH threshold at which future pore solutions would form.

It is also possible that there are additional water sources available to provide moisture to the salt patches, such as precipitation, snow melt, or groundwater. We reject this hypothesis due to the nearly synchronous changes in salt patch albedo across the cliff surface, on surfaces within

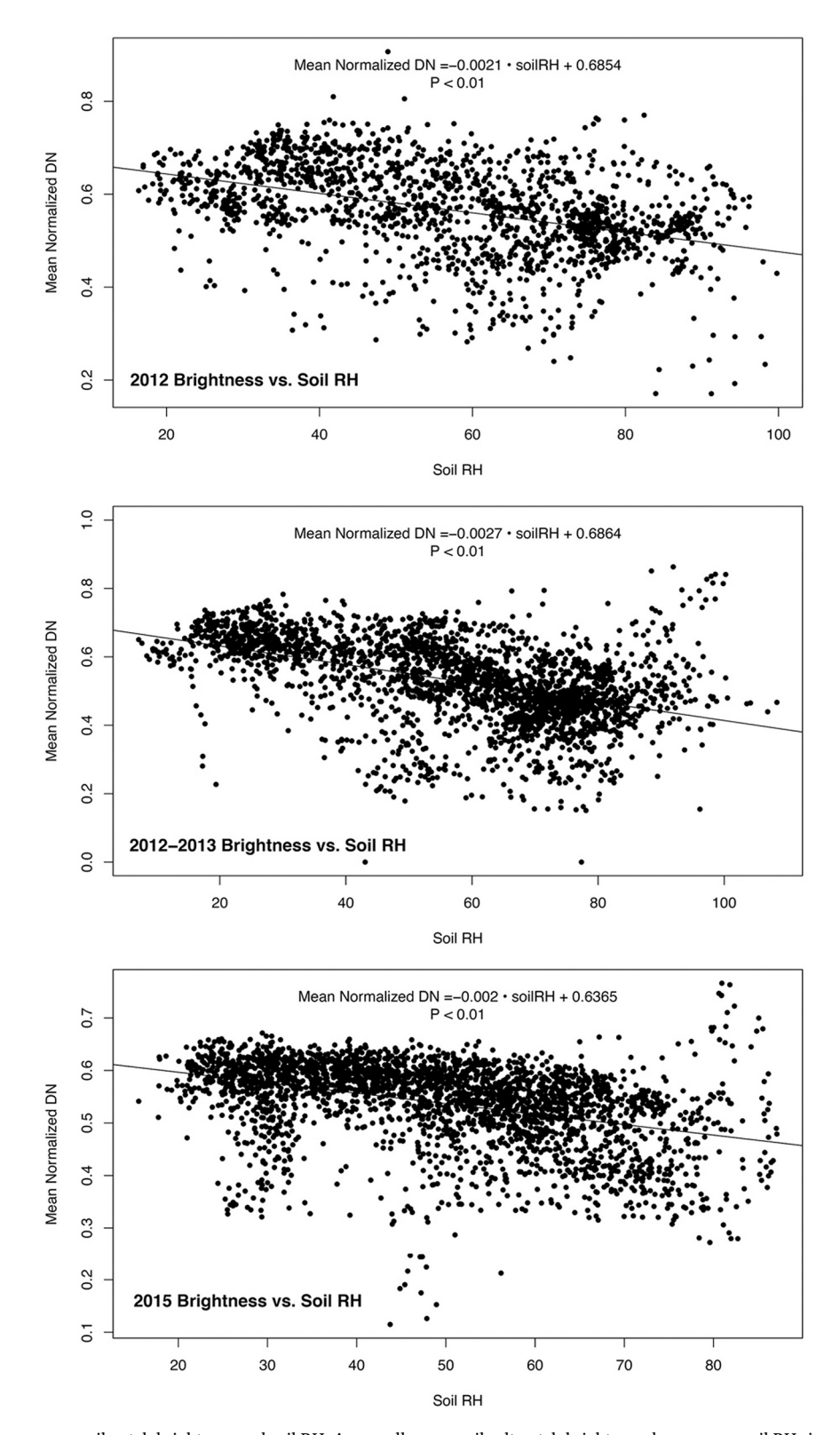


Fig. 10. Correlation between mean soil patch brightness and soil RH. Across all years, soil salt patch brightness decreases as soil RH rises. Best fit lines (least squares regression) are significant across all years, indicating that soil relative humidity and surface brightness are correlated. High surface brightness at high soil RH are snow events.

gully drainages and on interfluves, on surfaces near the exposed ice and distal from it. These nearly synchronous changes suggest that some orientation-dependent variable (e.g., boundary layer RH, insolation, soil temperature) are controlling albedo change, but that subsurface generation and transport of meltwater, which would be heterogeneous across

the hillslope, do not drive albedo change. We do not see evidence of surface runoff interacting with the salt patches, or evidence of subsurface flow moving past the salt patches.

Ultimately, salt crust formation is a dynamic process, which reflects the balance between evaporation, solute transport, and deliquescence

within a thin lens of the soil surface. Differences in humidity, salt content, and evaporation rate can drive salt crusts to migrate away from wetted soil surfaces at rates of up to 5  $\mu$ m/h (Dai et al., 2016), as salts dissolve at the wetted soil surface, are wicked up through the salt matrix by capillary action, and redeposit at the dry, air-exposed and illuminated top surface. Salt crusts at the Garwood ice cliff site are short lived and highly dynamic, undergoing multiple cycles of efflorescence and deliquescence or dissolution each austral summer. Conservatively, only considering times when the surface RH exceeds 79.9%, fully deliquesced conditions would be expected at the Garwood site for multiple hours every summer, predominantly during evening and "night" periods (Fig. 11) when the steep-walled site is fully in shadow.

The timing of albedo change at the ice cliff provides insight into the rates at which morphological and/or salt state change can occur. In all three field seasons, the surface albedo of salt patches fluctuates between dark and bright states. At the scale of the entire cliff, the albedo of spatially isolated patches changes in near unison. Differences in the rate of change between albedo state for most patches are within one frame (5 min), suggesting that each patch is broadly similar in salt composition and concentration and that similar RH conditions persist over the full  $\sim\!100$  m of the ice cliff hillslope. It is notable, however, that the albedo change is particularly rapid in the field; deliquescence can take hours at the salt grain scale under experimental conditions (Cohen et al., 1987). The patchiness of the bright salt deposits during their effloresced state suggests that many of the surrounding dry soils at the site lack concentrated salts.

# 4.4. Implications for the interpretation and analysis of RSL or other putative aqueous soil features in planetary environments?

A plethora of experimental studies have demonstrated that salts present on Mars, such as magnesium and calcium perchlorates of chlorides, are highly deliquescent (Hecht, 2002; Rennó et al., 2009; Smith et al., 2009). Deliquescence can result in brine formation, and some salts may produce solutions that could be metastable on the martian surface (e.g., Gough et al., 2017; Heinz et al., 2016; Nuding et al., 2014; Wang et al., 2019). While salt deliquescence has been proposed as a direct (Wang et al., 2019; McEwen et al., 2011) or indirect (Bishop et al., 2021) mechanism to trigger seasonal surface darkening associated with RSL,

direct identification of hydrated salt phases at RSL sites (Ojha et al., 2015) has proven challenging (Leask et al., 2018).

Our time lapse study shows that observations indicating wetting, or potentially even mineral hydration, are strongly dependent on the time of day that observations are made due to topographic control on microclimate conditions; shading during local "night" conditions cools the surface and raises soil RH, while the north-facing soil surface warms strongly during "daytime" illumination, causing humidity to drop above the soils and causing salts to effloresce. In comparison, over Mars, HiRISE is in a later afternoon orbit, providing images at around 15:00 local solar time (McEwen et al., 2010). If this same afternoon imaging pattern were used to observe the salt patches at the Garwood ice cliff site, even if imagery could be collected every day, wetted conditions would only be observed in a small minority of images (Fig. 12). For example, of the 18 days imaged during the 2012 field season, the ice cliff salts would have been fully deliquesced only in 2 of the 18 local afternoons, and deliquesced or both deliquesced and effloresced in 4 of the 18 afternoons. For the majority of the field season (12 of the 18 days). the cliff would have appeared as unchangingly bright if imaged only during the local afternoon.

Observational constraints from orbiting sensors challenge our ability to understand dynamic landscape processes that may move water through polar and planetary soils on timescales of minutes to hours, and that undergo both diel and seasonal secular changes. At the Garwood ice cliff site, it is unsurprising that soil salts deliquesce and that the resultant pore solutions darken the soil, but it is notable that this process reverses itself on daily timescales over transition periods lasting only minutes, and that bright, hydrated efflorescent salts may be masked by possible dehydration into anhydrous phases when daily and/or seasonal RH drops.

#### 5. Conclusions

Here we provide evidence that salty soil patches on the surface of Garwood ice cliff site produce dynamic albedo behavior. Tens of episodes of brightening and darkening, interpreted as evidence of deliquescence and efflorescence are observable in time-lapse images for each of the three field seasons studied. Simultaneous ground-level soil relative humidity measurements provide evidence for the extraction of

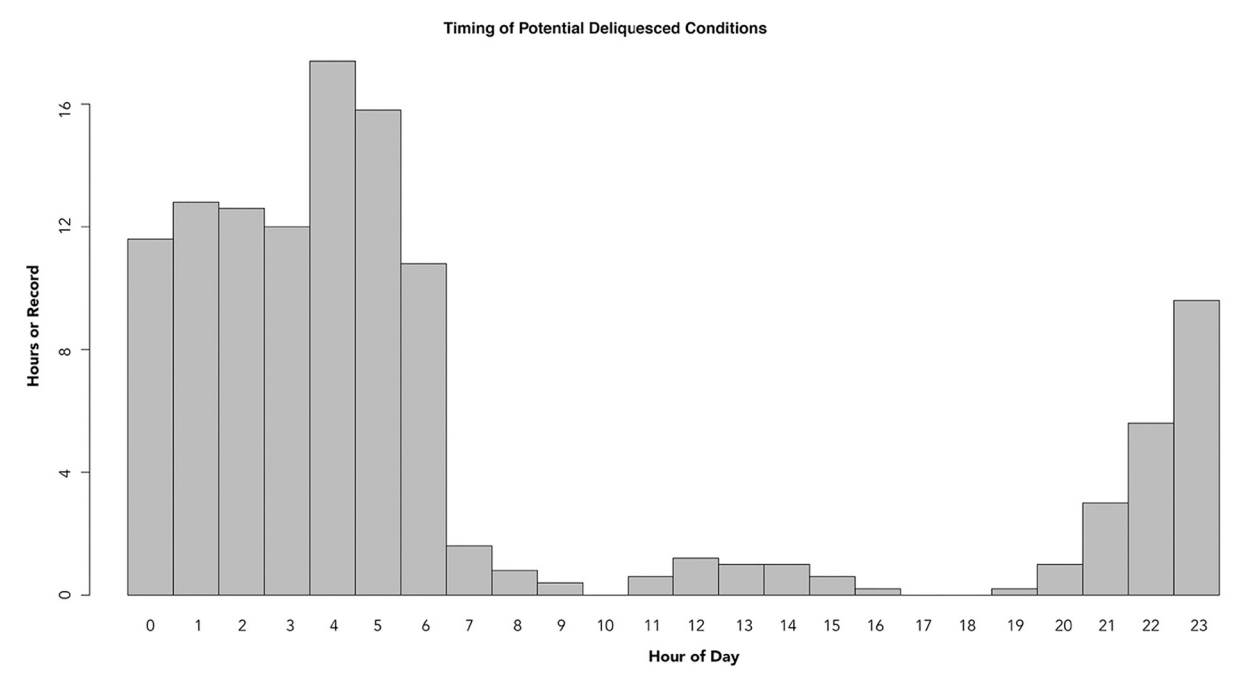


Fig. 11. Hours during the record for which surface RH > 79.9% plotted against hour of the day during which these conditions are present.

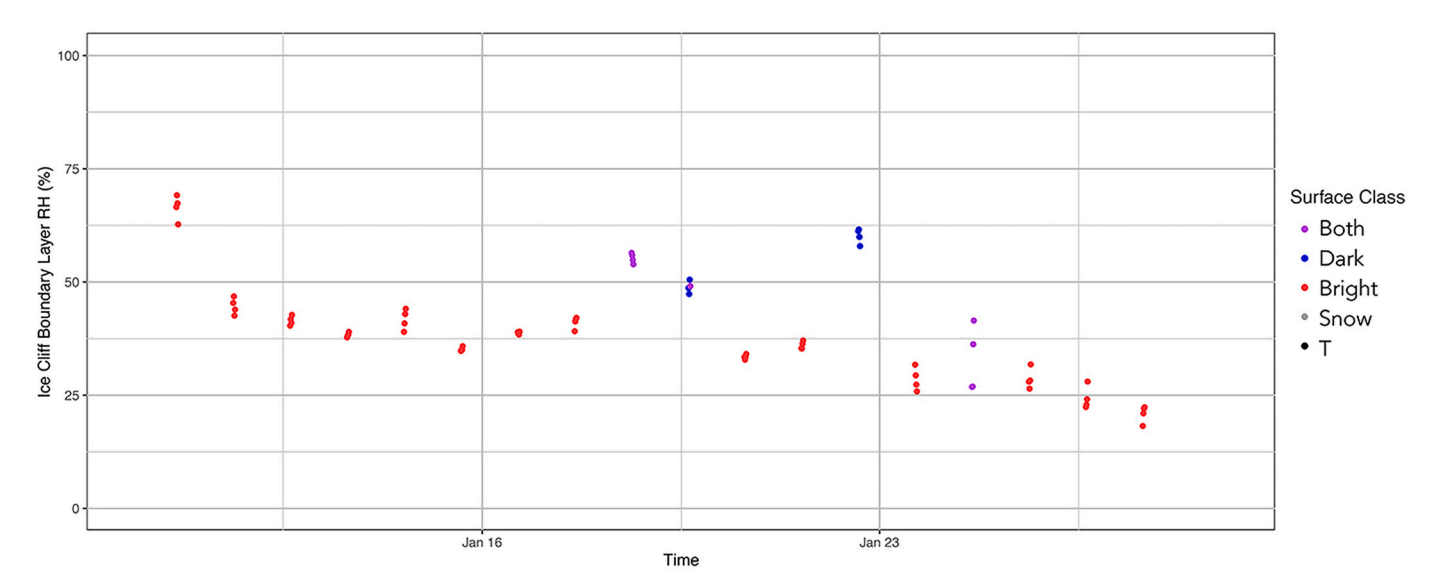


Fig. 12. Time series of RH values for the 2011–2012 imaging campaign, filtered only for 15:00–16:00 local time observations. If only afternoon images are considering, the ice cliff site patches are dominated by bright conditions, with darkened and both bright and dark conditions only visible in a handful of images.

atmospheric water vapor into deliquescing salt patches during periods of high RH and subsequent efflorescence of soil salt patches during periods of reduced surface RH. We show that deliquescence of salts is a mechanism for generating soil brines in the MDV over daily, seasonal, and inter-annual timescales. Further, we show Changes in salt expression on the surface can occur as quickly as 5 min. The deliquescence and efflorescence of salts are well-correlated with atmospheric RH. In general, the surface albedo of salt patches decreases when the humidity rises, indicating that moisture is being absorbed from the atmosphere. When the humidity decreases, the surface albedo increases as moisture is lost and the salts effloresce. The exact site-wide thresholds for deliquescence and efflorescence cannot be predicted in the same fashion as they are in a laboratory setting. This could be due to heterogeneity of salts, hydration state, salt concentration within the patch itself, or due to external environmental factors such as net radiation differentially warming or drying different portions of the hillslope.

The deliquescence of soil salts is a possible mechanism for generating brine on the surface of Mars. Low-albedo RSL could form through the interaction of hygroscopic salts and the martian atmosphere, with or without the presence of a flowing liquid water. However, wetting for extended periods of the martian day may be masked during low RH afternoon periods, as occurs for the salt patches in the MDV, which typically appear as non-wetted during the local afternoon. Thus, if RSL on Mars act like the salt patches documented here in the MDV, then the late afternoon HiRISE observations of RSL would not be expected to capture high-temporal albedo changes associated with RH darkening and brightening on diurnal timescales. Continuous, in situ imaging or sensor observation is essential for understanding the deliquescence and efflorescence behaviors of soil salt patches due to the rapid (minutes to hours) changes observed in soil wetness and albedo.

### **Declaration of Competing Interest**

None.

## Acknowledgements

This work was supported in part by the National Science Foundation under grants OPP-1847067 and OPP-1343835 to JSL.

#### Appendix A. Supplementary data

Supplementary data to this article can be found online at https://doi.org/10.1016/j.icarus.2022.114990.

#### References

Ball, B.A., Levy, J., 2015. The role of water tracks in altering biotic and abiotic soil properties and processes in a polar desert in Antarctica. J. Geophys. Res. Biogeosci. 120, 270–279. https://doi.org/10.1002/2014JG002856.

Ball, B.A., Virginia, R.A., 2012. Meltwater seep patches increase heterogeneity of soil geochemistry and therefore habitat suitability. Geoderma 189–190, 652–660. https://doi.org/10.1016/j.geoderma.2012.06.028.

Bao, H., Marchant, D.R., 2006. Quantifying sulfate components and their variations in soils of the McMurdo Dry Valleys, Antarctica. J. Geophys. Res.-Atmos. 111 https:// doi.org/10.1029/2005JD006669.

Bishop, J.L., Yeşilbaş, M., Hinman, N.W., Burton, Z.F.M., Englert, P.A.J., Toner, J.D., McEwen, A.S., Gulick, V.C., Gibson, E.K., Koeberl, C., 2021. Martian subsurface cryosalt expansion and collapse as trigger for landslides. Sci. Adv. 7, eabe4459. https://doi.org/10.1126/sciadv.abe4459.

Bisson, K.M., Welch, K.A., Welch, S.A., Sheets, J.M., Lyons, W.B., Levy, J.S., Fountain, A. G., 2015. Patterns and processes of salt efflorescences in the McMurdo region, Antarctica. Arct. Antarct. Alp. Res. 47, 407–425. https://doi.org/10.1657/AAAR0014-024.

Carns, R.C., Light, B., Warren, S.G., 2016. The spectral albedo of sea ice and salt crusts on the tropical ocean of Snowball Earth: II. Optical modeling. J. Geophys. Res. Oceans 121. 5217–5230. https://doi.org/10.1002/2016JC011804.

Claridge, G., Campbell, I.B., 1977. The salts in Antarctic soils, their distribution and relationship to soil processes. Soil Sci. 123, 377–384.

Cohen, M.D., Flagan, R.C., Seinfeld, J.H., 1987. Studies of concentrated electrolyte solutions using the electrodynamic balance. 2. Water activities for mixed-electrolyte solutions. J. Phys. Chem. 91, 4575–4582. https://doi.org/10.1021/j100301a030.

Craft, K.M., Horel, J.D., 2019. Variations in surface albedo arising from flooding and desiccation cycles on the Bonneville Salt Flats, Utah. J. Appl. Meteorol. Climatol. 58, 773–785. https://doi.org/10.1175/JAMC-D-18-0219.1.

Dai, S., Shin, H., Santamarina, J.C., 2016. Formation and development of salt crusts on soil surfaces. Acta Geotech. 11, 1103–1109. https://doi.org/10.1007/s11440-015-01011.

Davila, A.F., Gómez-Silva, B., de los Rios, A., Ascaso, C., Olivares, H., McKay, C.P., Wierzchos, J., 2008. Facilitation of endolithic microbial survival in the hyperarid core of the Atacama Desert by mineral deliquescence, 113, G01028. https://doi.org/ 10.1029/2007JG000561.

Davila, A.F., Duport, L.G., Melchiorri, R., Jänchen, J., Valea, S., de los Rios, A., Fairén, A. G., Möhlmann, D., McKay, C.P., Ascaso, C., 2010. Hygroscopic salts and the potential for life on Mars. Astrobiology 10, 617–628.

Davila, A.F., Hawes, I., Ascaso, C., Wierzchos, J., 2013. Salt deliquescence drives photosynthesis in the hyperarid Atacama Desert. Environ. Microbiol. Rep. 5, 583–587. https://doi.org/10.1111/1758-2229.12050.

Dickinson, W.W., Rosen, M.R., 2003. Antarctic permafrost: an analogue for water and diagenetic minerals on Mars. Geology 31, 199–202.

Dickson, J.L., Head, J.W., Levy, J.S., Marchant, D.R., 2013. Don Juan pond, Antarctica: near-surface CaCl2-brine feeding Earth's most saline lake and implications for Mars. Sci. Rep. 3 https://doi.org/10.1038/srep01166.

- Dickson, J.L., Levy, J.S., Head, J.W., 2014. Time-lapse imaging in polar environments. EOS Trans. Am. Geophys. Union 95, 1–2. https://doi.org/10.3189/ 002214310793146313
- Dundas, C.M., McEwen, A.S., Chojnacki, M., Milazzo, M.P., Byrne, S., McElwaine, J.N., Urso, A., 2017. Granular flows at recurring slope lineae on Mars indicate a limited role for liquid water. Nat. Geosci. 1–6 https://doi.org/10.1038/s41561-017-0012-5.
- Edwards, Christopher S., Piqueux, Sylvain, 2016. The water content of recurring slope lineae on Mars. Geophys. Res. Lett. 43 (17), 8912–8919.
- Fountain, A.G., Levy, J.S., Gooseff, M.N., Van Horn, D., 2014. The McMurdo Dry Valleys: A landscape on the threshold of change. Geomorphology 225, 25–35. https://doi. org/10.1016/j.geomorph.2014.03.044.
- Fountain, A.G., Nylen, T.H., Monaghan, A., Basagic, H.J., Bromwich, D., 2009. Snow in the McMurdo Dry Valleys, Antarctica. Int. J. Climatol. 30, 633–642. https://doi.org/ 10.1002/joc.1933.
- Gooseff, M.N., McKnight, D.M., Runkel, R.L., Vaughn, B.H., 2003. Determining long time-scale hyporheic zone flow paths in Antarctic streams. Hydrol. Process. 17, 1691–1710. https://doi.org/10.1002/hyp.1210.
- Gooseff, M.N., Barrett, J.E., Adams, B.J., Doran, P.T., Fountain, A.G., Lyons, W.B., McKnight, D.M., Priscu, J.C., Sokol, E.R., Takacs-Vesbach, C., Vandegehuchte, M.L., Virginia, R.A., Wall, D.H., 2017. Decadal ecosystem response to an anomalous melt season in a polar desert in Antarctica. Nature Ecol. Evol. 1, 1334–1338. https://doi.org/10.1038/s41559-017-0253-0.
- Gough, R.V., Wong, J., Dickson, J.L., Levy, J.S., Head, J.W., Marchant, D.R., Tolbert, M. A., 2017. Brine formation via deliquescence by salts found near Don Juan Pond, Antarctica: laboratory experiments and field observational results. Earth Planet. Sci. Lett. 476, 189–198. https://doi.org/10.1016/j.epsl.2017.08.003.
- Gough, Raina V., Nuding, D.L., Archer Jr., P.D., Fernanders, M.S., Guzewich, S.D., Tolbert, M.A., Toigo, A.D., 2020. Changes in soil cohesion due to water vapor exchange: a proposed dry-flow trigger mechanism for recurring slope lineae on Mars. Geophys. Res. Lett. 47, 11. https://doi.org/10.1029/2020GL087618.
- Grimm, R.E., Harrison, K.P., Stillman, D.E., 2013. Water budgets of martian recurring slope lineae. Icarus 1–12. https://doi.org/10.1016/j.icarus.2013.11.013.
- Harris, K.J., Carey, A.E., Lyons, W.B., Welch, K.A., Fountain, A.G., 2007. Solute and isotope geochemistry of subsurface ice melt seeps in Taylor Valley, Antarctica. Geol. Soc. Am. Bull. 119, 548–555. https://doi.org/10.1130/B25913.1.
- Hecht, M., 2002. Metastability of liquid water on mars. Icarus 156, 373–386. https://doi. org/10.1006/jcar.2001.6794.
- Hecht, M.H., Kounaves, S.P., Quinn, R.C., West, S.J., Young, S.M.M., Ming, D.W., Catling, D.C., Clark, B.C., Boynton, W.V., Hoffman, J., DeFlores, L.P., Gospodinova, K., Kapit, J., Smith, P.H., 2009. Detection of perchlorate and the soluble chemistry of Martian soil at the Phoenix Lander site. Science. https://doi.org/10.1126/science.1172466.
- Heinz, J., Schulze-Makuch, D., Kounaves, S.P., 2016. Deliquescence-induced wetting and RSL-like darkening of a Mars analogue soil containing various perchlorate and chloride salts. Geophys. Res. Lett. 43, 4880–4884. https://doi.org/10.1002/ 2016GL068919.
- Huang, J., 2018. A simple accurate formula for calculating saturation vapor pressure of water and ice. J. Appl. Meteorol. Climatol. 57 (6), 1265–1272. https://doi.org/ 10.1175/JAMC-D-17-0334-1.
- Huber, C., Ojha, L., Lark, L., Head, J.W., 2020. Physical models and predictions for recurring slope lineae formed by wet and dry processes. Icarus 335, 113385. https:// doi.org/10.1016/j.icarus.2019.07.019.
- Keys, J.R., 1979. Distribution of salts in the McMurdo region, with analyses from the saline discharge area at the terminus of Taylor Glacier. PhD Thesis. University of Wellington.
- Keys, J.R., Williams, K., 1981. Origin of crystalline, cold desert salts in the Mcmurdo Region, Antarctica. Geochim. Cosmochim. Acta 45, 2299–2309.
- Koop, T., Kapilashrami, A., Molina, L.T., Molina, M.J., 2000. Phase transitions of seasalt/water mixtures at low temperatures: implications for ozone chemistry in the polar marine boundary layer. J. Geophys. Res.-Atmos. 105, 26393–26402. https:// doi.org/10.1029/2000JD900413.
- Lark, L.H., Huber, C., Head, J.W., 2021. Anomalous recurring slope lineae on Mars: implications for formation mechanisms. Icarus 357, 114129. https://doi.org/ 10.1016/j.icarus.2020.114129.
- Leask, E.K., Ehlmann, B.L., Dundar, M.M., Murchie, S.L., Seelos, F.P., 2018. Challenges in the search for perchlorate and other hydrated minerals with 2.1-µm absorptions on Mars. Geophys. Res. Lett. 45 https://doi.org/10.1029/2018GL080077, 151–10.
- Levy, J., 2012. Hydrological characteristics of recurrent slope lineae on Mars: evidence for liquid flow through regolith and comparisons with Antarctic terrestrial analogs. Icarus 219, 1–4. https://doi.org/10.1016/j.icarus.2012.02.016.
- Levy, J.S., 2021. Episodic basin-scale soil moisture anomalies associated with high relative humidity events in the McMurdo Dry Valleys, Antarctica. Antarct. Sci. 33 (5), 533–547.
- Levy, J.S., Fountain, A.G., Gooseff, M.N., Welch, K.A., Lyons, W.B., 2011. Water tracks and permafrost in Taylor Valley, Antarctica: extensive and shallow groundwater connectivity in a cold desert ecosystem. Geol. Soc. Am. Bull. 123, 2295–2311. https://doi.org/10.1130/B30436.1.
- Levy, J.S., Fountain, A.G., Welch, K.A., Lyons, W.B., 2012. Hypersaline "wet patches" in Taylor Valley, Antarctica. Geophys. Res. Lett. 39 https://doi.org/10.1029/ 2012GL050898.
- Levy, Joseph S., Fountain, A.G., O'Connor, J.E., Welch, K.A., Lyons, W.B., 2013. Garwood Valley, Antarctica: a new record of last glacial maximum to Holocene glacio-fluvial processes in the McMurdo Dry Valleys. Geol. Soc. Am. Bull. 125, 1484–1502.

Levy, J., Fountain, A., Lyons, W.B., Welch, K., 2014. Experimental formation of pore fluids in McMurdo Dry Valleys soils. Antarct. Sci. 1–9 https://doi.org/10.1017/ S0954102014000479.

- Levy, J.S., Rittenour, T.M., Fountain, A.G., O'Connor, J.E., 2017. Luminescence dating of paleolake deltas and glacial deposits in Garwood Valley, Antarctica: implications for climate, Ross ice sheet dynamics, and paleolake duration. Geol. Soc. Am. Bull. https://doi.org/10.1130/B31539.1. B31539.1-14.
- Lyons, W.B., Welch, K.A., Carey, A.E., Doran, P.T., Wall, D.H., Virginia, R.A., Fountain, A.G., Csatho, B.M., Tremper, C.M., 2005. Groundwater seeps in Taylor Valley Antarctica: an example of a subsurface melt event. Ann. Glaciol. 40, 200–206.
- Marchant, D.R., Head, J.W., 2007. Antarctic dry valleys: microclimate zonation, variable geomorphic processes, and implications for assessing climate change on Mars. Icarus 192, 187–222. https://doi.org/10.1016/j.icarus.2007.06.018.
- Martin, S.T., 2000. Phase transitions of aqueous atmospheric particles. Chem. Rev. 100, 3403–3454. https://doi.org/10.1021/cr990034t.
- Massé, M., Beck, P., Schmitt, B., Pommerol, A., McEwen, A., Chevrier, V.F., Brissaud, O., 2012. Nature and origin of RSL: spectroscopy and detectability of liquid brines in the near-infrared. Lunar Planetary Instit. Sci. Conf. Abstracts 43, 1856.
- McEwen, A.S., Banks, M.E., Baugh, N., Becker, K., Boyd, A., Bergstrom, J.W., Beyer, R.A., Bortolini, E., Bridges, N.T., Byrne, S., Castalia, B., Chuang, F.C., Crumpler, L.S., Daubar, I., Davatzes, A.K., Deardorff, D.G., DeJong, A., Alan Delamere, W., Dobrea, E.N., Dundas, C.M., Eliason, E.M., Espinoza, Y., Fennema, A., Fishbaugh, K. E., Forrester, T., Geissler, P.E., Grant, J.A., Griffes, J.L., Grotzinger, J.P., Gulick, V.C., Hansen, C.J., Herkenhoff, K.E., Heyd, R., Jaeger, W.L., Jones, D., Kanefsky, B., Keszthelyi, L., King, R., Kirk, R.L., Kolb, K.J., Lasco, J., Lefort, A., Leis, R., Lewis, K. W., Martinez-Alonso, S., Mattson, S., McArthur, G., Mellon, M.T., Metz, J.M., Milazzo, M.P., Milliken, R.E., Motazedian, T., Okubo, C.H., Ortiz, A., Philippoff, A.J., Plassmann, J., Polit, A., Russell, P.S., Schaller, C., Searls, M.L., Spriggs, T., Squyres, S.W., Tarr, S., Thomas, N., Thomson, B.J., Tornabene, L.L., Van Houten, C., Verba, C., Weitz, C.M., Wray, J.J., 2010. The High Resolution Imaging Science Experiment (HiRISE) during MRO's Primary Science Phase (PSP). Icarus 205, 2–37. https://doi.org/10.1016/j.icarus.2009.04.023.
- McEwen, A.S., Ojha, L., Dundas, C.M., Mattson, S.S., S, B, 2011. Seasonal flows on warm Martian slopes. Science 333, 740–743.
- McEwen, A.S., Schaefer, E.I., Dundas, C.M., Sutton, S.S., Tamppari, L.K., Chojnacki, M., 2021. Mars: abundant recurring slope lineae (RSL) following the planet-encircling dust event (PEDE) of 2018. J. Geophys. Res. Planets 126. https://doi.org/10.1029/2020JE006575 e2020JE006575.
- McKay, C.P., Friedmann, E.I., Gomez-Silva, B., Caceres-Villanueva, L., Andersen, D.T., Landheim, R., 2003. Temperature and moisture conditions for life in the extreme arid region of the Atacama Desert: four years of observations including the El Nino of 1997–1998. Astrobiology 3, 393–406. https://doi.org/10.1089/ 1531102033769016460
- Murchie, S., Arvidson, R., Bedini, P., Beisser, K., Bibring, J.P., Bishop, J., Boldt, J., Cavender, P., Choo, T., Clancy, R.T., Darlington, E.H., 2007. Compact reconnaissance imaging spectrometer for Mars (CRISM) on Mars reconnaissance orbiter (MRO). J. Geophys. Res. Planets 112 (E5).
- Nishiyama, T., Kurasawa, H., 1975. Distribution of secondary minerals from Taylor Valley. Dry Valley Drilling Project Bulletin. 120–133.
- Nuding, D.L., Rivera-Valentin, E.G., Davis, R.D., Gough, R.V., Chevrier, V.F., Tolbert, M. A., 2014. Deliquescence and efflorescence of calcium perchlorate: an investigation of stable aqueous solutions relevant to Mars. Icarus 243, 420–428. https://doi.org/10.1016/j.icarus.2014.08.036.
- Ojha, L., Wilhelm, M.B., Murchie, S.L., McEwen, A.S., Wray, J.J., Hanley, J., Massé, M., Chojnacki, M., 2015. Spectral evidence for hydrated salts in recurring slope lineae on Mars. Nat. Geosci. https://doi.org/10.1038/ngeo2546.
- Osterloo, M.M., Hamilton, V.E., Bandfield, J.L., Glotch, T.D., Baldridge, A.M., Christensen, P.R., Tornabene, L.L., Anderson, F.S., 2008. Chloride-bearing materials in the southern highlands of Mars. Science 319, 1651–1654. https://doi.org/10.1126/science.1150690
- Rennó, N.O., Bos, B.J., Catling, D., Clark, B.C., Drube, L., Fisher, D., Goetz, W., Hviid, S. F., Keller, H.U., Kok, J.F., Kounaves, S.P., Leer, K., Lemmon, M., Madsen, M.B., Markiewicz, W.J., Marshall, J., McKay, C., Mehta, M., Smith, M., Zorzano, M.P., Smith, P.H., Stoker, C., Young, S.M.M., 2009. Possible Physical and Thermodynamical Evidence for Liquid Water at the Phoenix Landing Site 114, E00E03. https://doi.org/10.1029/2009JE003362.
- Rodriguez-Navarro, C., Doehne, E., 1999. Salt weathering: influence of evaporation rate, supersaturation and crystallization pattern. Earth Surf. Process. Landf. 24, 191–209. https://doi.org/10.1002/(SICI)1096-9837(199903)24:3<191::AID-ESP942>3.0. CO-2-G
- Sato, M., Hattanji, T., 2018. A laboratory experiment on salt weathering by humidity change: salt damage induced by deliquescence and hydration. Prog. Earth Planet Sci. 5, 84. https://doi.org/10.1186/s40645-018-0241-2.
- Schmidt, F., Andrieu, F., Costard, F., Kocifaj, M., Meresescu, A.G., 2017. Formation of recurring slope lineae on Mars by rarefied gas-triggered granular flows. Nat. Geosci. 10, 270–273. https://doi.org/10.1038/ngeo2917.
- Schwerdtfeger, W., 1984. Weather and climate of the Antarctic. Dev. Atmos. Sci. 15. Smith, P.H., Tamppari, L.K., Arvidson, R.E., Bass, D., Blaney, D., Boynton, W., Carswell, A., Catling, D.C., Clark, B.C., Duck, T., DeJong, E., Fisher, D., Goetz, W., Gunnlaugsson, H.P., Hecht, M.H., Hipkin, V., Hoffman, J., Hviid, S.F., Keller, H.U., Kounaves, S.P., Lange, C.F., Lemmon, M.T., Madsen, M.B., Markiewicz, W.J., Marshall, J., McKay, C.P., Mellon, M.T., Ming, D.W., Morris, R.V., Pike, W.T., Renno, N., Staufer, U., Stoker, C., Taylor, P., Whiteway, J.A., Zent, A.P., 2009. H2O at the phoenix landing site. Science 325, 58–61.

- Steiger, M., Asmussen, S., 2008. Crystallization of sodium sulfate phases in porous materials: the phase diagram Na2SO4–H2O and the generation of stress. Geochim. Cosmochim. Acta 72, 4291–4306. https://doi.org/10.1016/j.gca.2008.05.053.
- Stillman, D.E., Michaels, T.I., Grimm, R.E., Hanley, J., 2016. Observations and modeling of northern mid-latitude recurring slope lineae (RSL) suggest recharge by a presentday martian briny aquifer. Icarus 265, 125–138. https://doi.org/10.1016/j. icarus 2015 10.007
- Stillman, David E., Bue, Brian D., Wagstaff, Kiri L., Primm, Katherine M., Michaels, Tim I., Grimm, Robert E., 2020. Evaluation of wet and dry recurring slope lineae (RSL) formation mechanisms based on quantitative mapping of RSL in Garni crater, Valles Marineris, Mars. Icarus 335. https://doi.org/10.1016/j.icarus.2019.113420.
- Stuiver, M., Denton, G.H., Hughes, T.J., Fastook, J.L., 1981. History of the marine ice sheet in West Antarctica during the last glaciation: a working hypothesis. In: Denton, G.H., Hughes, T.J. (Eds.), The Last Great Ice Sheets. John Wiley & Sons, New York, NY, pp. 319–362.
- Tang, I.N., Munkelwitz, H.R., 1993. Composition and temperature dependence of the deliquescence properties of hygroscopic aerosols. Atmos. Environ. Part A 27, 467–473. https://doi.org/10.1016/0960-1686(93)90204-C.
- Tebolt, M., Levy, J., Goudge, T., Schorghofer, N., 2020. Slope, elevation, and thermal inertia trends of martian recurring slope lineae initiation and termination points: multiple possible processes occurring on coarse, sandy slopes. Icarus 338. https:// doi.org/10.1016/j.icarus.2019.113536, 113536–12.

- Toner, J.D., Sletten, R.S., 2013. The formation of ca-cl-rich groundwaters in the dry valleys of Antarctica: field measurements and modeling of reactive transport. Geochim. Cosmochim. Acta 110, 84–105. https://doi.org/10.1016/j. gca.2013.02.013.
- Toner, J.D., Sletten, R.S., Prentice, M.L., 2013. Soluble salt accumulations in Taylor Valley, Antarctica: implications for paleolakes and Ross Sea Ice Sheet dynamics. J. Geophys. Res. Earth Surf. 118, 198–215.
- Wang, A., Ling, Z., Yan, Y., McEwen, A.S., Mellon, M.T., Smith, M.D., Jolliff, B.L., Head, J., 2019. Subsurface cl-bearing salts as potential contributors to recurring slope lineae (RSL) on Mars. Icarus 333, 464–480. https://doi.org/10.1016/j. icarus.2019.06.024.
- Wise, M.E., Baustian, K.J., Koop, T., Freedman, M.A., Jensen, E.J., Tolbert, M.A., 2012. Depositional ice nucleation onto crystalline hydrated NaCl particles: a new mechanism for ice formation in the troposphere. Atmos. Chem. Phys. 12, 1121–1134. https://doi.org/10.5194/acp-12-1121-2012.
- Yang, L., Pabalan, R.T., Juckett, M.R., 2006. Deliquescence relative humidity measurements using an electrical conductivity method. J. Solut. Chem. 35, 583–604. https://doi.org/10.1007/s10953-005-9015-8.
- Zehnder, K., Schoch, O., 2008. Efflorescence of mirabilite, epsomite and gypsum traced by automated monitoring on-site. J. Cult. Herit. https://doi.org/10.1016/j. culher.2008.10.009.